MNRAS **000**, 1–?? (2018) Preprint 26 January 2019 Compiled using MNRAS LATEX style file v3.0

The expected shape of the Milky Way's Dark Matter halo

Jesus Prada,[1⋆] Jaime E. Forero-Romero,[1] Volker Springel[2]
[1] *Departamento de Fśica, Universidad de los Andes, Cra. 1 No. 18A-10, Edificio Ip, Bogot; Colombia.*
[2] *Heidelberg Institute for Theoretical Studies, Schloss-Wolfsbrunnenweg 35, D-69118 Heidelberg Germany.*

Accepted XXX. Received YYY; in original form ZZZ

ABSTRACT
We measure the shape of the dark matter halos of Milky Way type galaxies.

Key words: keyword1 – keyword2 – keyword3

1 INTRODUCTION

A robust prediction of the Cold Dark Matter (CDM) paradigm is that DM halos are ellipsoidal and can be characterized by the principal axes $a > b > c$. This ellipsoidal shape is mostly due to the anisotropical and clumpy accretion of matter influenced by environmental structures. Numerical studies how that the shape has a strong mass dependence (Allgood et al. 2006), halos are also rounder at the outerskirts than at the inner part. Shape also evolves with cosmic time, halos get rounder as they evolve.

There is however a high degree of uncertainty on what is the degree of uncertainty on the degree of ellipticity of the Milky Way DM halo. This problem has been addressed both by observations and simulations. The difficulty in making an observational measurement lies in the indirect nature of the effect; i.e. the ellipticity can only be constrained by its effects on quantities such as stellar radial velocities. In simulations the uncertainty on predicting the MW DM ellipticity is driven by the different physical effects that should be modeled and its different possible numerical implementations.

Observationally some studies prefer oblate (i.e. a=b>c) configurations at small distances around $\leq$ 20 kpc (see Law & Majewski 2010; Bovy et al. 2016; Loebman et al. 2012; Olling & Merrifield 2000; Banerjee & Jog 2011) and more triaxial and prolate configurations on the outter distances $\geq$ 20 kpc (see Vera-Ciro & Helmi 2013; Law et al. 2009; Deg & Widrow 2013; Banerjee & Jog 2011). However, some studies are inclined towards prolate configurations even at the inner parts of the halo (see Bowden et al. 2016), and although it previously seemed that a triaxial DM halo on the outerskirts would be necessary to fully explain the characterization of the Sagittarius stream (Law et al. 2009), recent studies questioned this claim by reporting inconsistencies with narrow stellar streams Pearson et al. (2015) or finding that the relaxation of other constraints may make this claim unnecessary Ibata et al. (2013).

⋆ E-mail: jd.prada1760@uniandes.edu.co

In simulations there is strong evidence claiming that the presence of baryons produces axisymmetrical halos. For instance, some studies have shown that the DM halo shape must be axisymmetrical to ensure the stability of a hydrodynamical disk embeded in a static DM halo. Other have studied this rounding effect by simulating the disk as rigid potential inside an N-body triaxial DM halo Debattista et al. (2008); Debattista et al. (2013); Kazantzidis et al. (2010) finding that the halo responds to the disk by becoming less triaxial.

The caveat of the studies mentioned above is that they do not follow baryons in the whole cosmological context. Other studies overcome this limitation by using resimulations (Abadi et al. 2010; Bryan et al. 2013) finding that the feeback related to star formation in the disk drives the strenght of the round effect. Recently Chua et al. (2018a) made a study in a cosmological simulation to compare the effect of including baryons. They do find, on average, rounder halo shapes once hydrodynamic effects are included, but it is uncertain the strenght of this statistical effect on galaxies similar to the MW.

All these difficulties (enough numerical resolution, explicit cosmological context, appropriate feedback physics to produce realistic MW disks) have limited the studies that want to study the rounding effect of baryons in MW-like galaxies. In this work we overcome all these limitations by analyzing the results of state-of-the-art hydrodynamical simulations of isolated halos that resemble the Milky Way. We also perform a convergence study with simulation performed at different resolution levels and explicitly compare the role of DM only vs. DM+hydro on the MW DM halo shape.

2 NUMERICAL SIMULATIONS

In this work we use the results of the state-of-the art Auriga simulations (Grand et al. 2017). The objects in those simulations were selected from a set of 30 isolated halos in the Evolution and Assembly of GaLaxies and their Environments (EAGLE) project (Schaye et al. 2015). These halos were ran-

Reference	q_ρ	s_ρ	q_ϕ	s_ϕ	R	θ	comment
Olling & Merrifield (2000)	**1.00**	**0.80**			$\simeq$ 8kpc	0°	Method: Stellar dynamics and HI density.
Law et al. (2009)			**0.83**	**0.67**	$\lesssim$ 60kpc	90°	Mid-axis orientation. Method: Sagittarius stream
Law & Majewski (2010)			**0.99**	**0.72**	[20kpc,60kpc]	90°	Mid-axis orientation, Method: Sagittarius stream
Loebman et al. (2012)	**1.00**	**0.47**			$\sim$ 20kpc	0°	Method: SDSS statistics
Deg & Widrow (2013)	0.72	0.28	0.82	0.40	[20kpc,60kpc]	90°	Mid-axis orientation. Method: Sagittarius stream
Vera-Ciro & Helmi (2013)			**1.00** **0.90**	**0.90** **0.80**	$\lesssim$ 10kpc $\gtrsim$ 10kpc	0° 90°	Method: Sagittarius stream & LMC Mid-axis orientation on the outside.
Bovy et al. (2016)	**0.95**	**0.95**			$\lesssim$ 20kpc	90°	Method: Stellar streams
Bowden et al. (2016)			[**0.5**, **0.66**]	[**0.5**, **0.66**]	[5kpc,10kpc]	90°	Weak constraint on prolate halo. Method: SDSS stars dynamics.
Banerjee & Jog (2011)	**1** **0.5**	**1** **0.5**			9kpc 24kpc	0° 0°	Method: HI gas. Monotonical change between radial regimes.
Johnston et al. (2005)	**1**	[**0.83** – **0.92**]			$\lesssim$ 60kpc	0°	Method: Sagittarius stream

Table 1. (TODO: compute analogues in isopotential or isodensity according to Binney and Tremaine)

Reference	q_ρ	s_ρ	q_ϕ	s_ϕ	R	comment
Chua et al. (2018b)	**0.88** $\pm$ **0.10**	**0.70** $\pm$ **0.11**			$0.15R_{200}$	Illustris
Bryan et al. (2013)	[**0.84**, **0.86**]	[**0.66**, **0.70**]			R_{200}	For different cosmologies and feedback recipies. Calculated from a fit at $M_\odot = 10^12$
Abadi et al. (2010)			**0.98**	**0.85**	-	Almost independent of radius. No feedback: boundary case

Table 2. (TODO: compute analogues in isopotential or isodensity according to Binney and Tremaine)

domly selected from a sample of the most isolated quartile of halos whose virial mass M_{200} varied between $10^{12} M_\odot$ and $2 \times 10^{12} M_\odot$. These halos were re-simulated with higher resolution an varying physical realism using the AREPO code (Springel 2010).

All 30 halos were simulated within resolution defined for Aquarius simulations corresponding to $\sim 3 \times 10^6$ high resolution DM particles of $\sim 2.5 \times 10^5 M_\odot$. This resolution is labeled as Level 4, the main details for each halo are consigned in Table **??**. From these 30 halos, 6 of them where re-simulated at higher resolution (labeled as Level 3) taking into account a spatial factor of 2 in each dimension. Details of Level 3 halos are in Table **??**. Furthermore, for each halo in each level of resolution there are two versions of the simulation: DM-only and DM plus baryons with magneto-hydrodynamical (MHD) physics.

3 DETERMINING THE HALO SHAPE

There are two main ways to estimate the DM halo shape at a fixed radius: by computing isopotential or isodensity surfaces. Observational inference models estimate the shape from the isopotential contours, while simulations work with the isodensity contours which can be directly calculated from particle positions. However, the density contours are not smooth and are very sensitive to the presence of small satelites. For this reason we choose to measure the shape by taking volume-enclosed particles, rather than shell-enclosed.

We follow the shape measurement method presented by Allgood et al. (2006) that uses the reduced inertia tensor,

$$I_{ij} = \sum_k \frac{x_k^{(i)} x_k^{(j)}}{d_k^2}, \quad (1)$$

with the positions components weighted by the k-th particle distance $d_k^2 = x_k^2 + y_k^2 + z_k^2$, the particle positions are measured from the minimum of the gravitational potential in each halo. The diagonalization of this tensor yields the principal axes of the structure as well as the eigenquantities which are proportional to the squared principal axes $a > b > c$.

We start the calculations taking into account particles within a sphere of radius R and then recharacterize the triaxial parameters by taking into account particles within an ellipsoid of semi-axes $r, r/q, r/s$ and weighted distance $d^2 = x^2 + (y/q)^2 + (z/s)^2$, where $q = b/a$ and $s = c/a$ are the previously calculated axial ratios. We repeat this process until the average deviation of semi-axes is less than 10^{-6}. This is the same method used to estimate the halo shape in the DM-only Aquarius simulations (Vera-Ciro et al. 2011).

We restrict the sampling of the ellipsoidal parameters to radii between $1/16 R_{vir}$ and $2R_{vir}$, where R_{vir} is taken as the radius enclosing a sphere with 500 times the average dark

	$R_{1/16}$	$R_{1/8}$	$R_{1/4}$	$R_{1/2}$	R_1	R_2
$\bar{q}$	$0.55^{+0.07}_{-0.07}$	$0.57^{+0.09}_{-0.08}$	$0.61^{+0.15}_{-0.08}$	$0.65^{+0.18}_{-0.10}$	$0.70^{+0.13}_{-0.10}$	$0.75^{+0.10}_{-0.10}$
$\bar{s}$	$0.42^{+0.12}_{-0.03}$	$0.45^{+0.11}_{-0.04}$	$0.49^{+0.09}_{-0.05}$	$0.52^{+0.10}_{-0.05}$	$0.56^{+0.10}_{-0.05}$	$0.59^{+0.11}_{-0.06}$
$\bar{T}$	$0.89^{+0.03}_{-0.08}$	$0.88^{+0.04}_{-0.12}$	$0.84^{+0.08}_{-0.23}$	$0.81^{+0.08}_{-0.29}$	$0.75^{+0.14}_{-0.25}$	$0.71^{+0.16}_{-0.19}$

Table 3. Median values of axial ratios q, s and triaxiality parameter T for DM halos in DM-only simulations at different radii (columns).

	$R_{1/16}$	$R_{1/8}$	$R_{1/4}$	$R_{1/2}$	R_1	R_2
$\bar{q}$	$0.93^{+0.04}_{-0.04}$	$0.95^{+0.03}_{-0.03}$	$0.95^{+0.02}_{-0.05}$	$0.93^{+0.04}_{-0.06}$	$0.93^{+0.04}_{-0.10}$	$0.92^{+0.03}_{-0.09}$
$\bar{s}$	$0.73^{+0.05}_{-0.09}$	$0.73^{+0.07}_{-0.10}$	$0.73^{+0.08}_{-0.10}$	$0.73^{+0.09}_{-0.08}$	$0.75^{+0.07}_{-0.11}$	$0.74^{+0.07}_{-0.10}$
$\bar{T}$	$0.31^{+0.15}_{-0.22}$	$0.20^{+0.24}_{-0.12}$	$0.24^{+0.20}_{-0.12}$	$0.30^{+0.26}_{-0.16}$	$0.36^{+0.23}_{-0.23}$	$0.39^{+0.26}_{-0.13}$

Table 4. Median values of axial ratios q, s and triaxiality parameter T for DM halos in MHD simulations at different radii (columns).

matter density of the Universe. All our results use of this reference radius unless strictly stated otherwise. We peform the shape measurements both as a function of radius and redshift for all halos in the sample.

4 RESULTS

4.1 Radial trends

In DM-only simulations halos are monotonically rounder with increasing radius, this confirms results already reported in the literature (Vera-Ciro et al. 2011). Figure 1 illustrates this effect. There we show the DM density of a DM-only halo at redshift zero. The halo is aligned with the minor axis. The ellipsoid shows the outermost boundary of the estimated shape ellipsoid. Formally, this effect is reflected in the axial ratios $b/a, c/a$, which tend to unity on the outerskirts of the halo. As a representative sample of this relations, we show on figure **??** the evolution, for a specific halo, of the axial ratios $b/a, c/a$ and the triaxiality parameter $T = \frac{a^2-b^2}{a^2-c^2}$ in a wide range of radii.

4.2 The radial tendency of axial ratios

We found that most halos exhibit a monotonically-increasing somewhat steady tendency of its axial ratios $b/a, c/a$ with radius, which is well exemplified on figure **??**. There are some special cases in which fluctuations of the local DM density field affects this relation, but in average, this monotonic and steady tendency is clear and can be consulted on table **??**. To ilustrate the average behavior, as well as some peculiarities, we resume the results of the 30 auriga simulations on the figure **??** where each shape represents a point in the triaxiality plane c/a Vs b/a. Check Vera-ciro onthis.

Concerning MHD halos, *prescindible?(((the expected tendency is not clear. Some studies claim that the DM halo must be oblate, at least in the vicinities of the disk, to ensure its stability* **?**. *However,)))* not much is said about its dependence with radius as previous studies focus rather on the effects of baryons on the dynamics of the halo at fixed radii. Examining the representative behaviour of a MHD halo on figure **??**, some things are noticeable: first, the DM halo is almost perfectly oblate around $\approx 10-30$Kpc, second, its axial ratio b/a start decreasing very slowly after $50Kpc$ and below $10Kpc$ and third, its axial ratio c/a does not exhibit noticeable change in the whole radial domain. (Pass from representative case to averaged values) These results are statistically supported and sumarized on table **??** and figure **??**

	$R_{1/8}$	$R_{1/4}$	$R_{1/2}$	R_1
$\bar{q}$	$0.98^{+0.01}_{-0.02}$	$0.97^{+0.01}_{-0.04}$	$0.96^{+0.03}_{-0.06}$	$0.94^{+0.03}_{-0.07}$
$\bar{s}$	$0.89^{+0.04}_{-0.06}$	$0.88^{+0.04}_{-0.04}$	$0.87^{+0.05}_{-0.05}$	$0.85^{+0.05}_{-0.05}$
$\bar{T}$	$0.18^{+0.23}_{-0.10}$	$0.36^{+0.19}_{-0.21}$	$0.40^{+0.26}_{-0.20}$	$0.48^{+0.23}_{-0.21}$

Table 5. Median values of isopotential axial ratios q, s and triaxiality parameter T for DM halos in MHD simulations at different radii (columns).

4.3 Comparison with observational constraints

To be able to compare our results with observational values, we must relate the calculated quanties with their corresponding isopotential analogue, in which observational constraints are usually presented. For this purpose, we run a simple algorithm to find an approximation of the shape of the isopotential contour. Here, we calculate the mean and standard deviation of the potential over a spherical shell of width equals to 10% of the radius at which it is sampled. Then, we calculate the inertia tensor of particles with potential within 1σ around the mean potential and calculate its triaxial characterization with the reduced inertia tensor. We repeat the process of calculating the potential mean and standard deviation until convergence is achieved with tolerance of 10^{-4}. We repeat this process for the different radii from table **??**.

As a check of consistency, we compare our new isopotential shape results with the analytic expression of the $(1-q_\phi)\frac{1}{3}(1-q_\rho)$ (**?**, Binney and Tremaine year), taking the volume-enclosed axial ratios as an approximation for the isodensity contour ratios q_ρ. Although this analytic expression if meant to be used for logarithmic axisymmetric halos, it works well as a first approximation for nearly axisymmetric halos as those produced by our disced galaxies. We find that the difference between the real and the analytic isopotential axial ratios is not bigger than *quantitypercent*. With this, we may now present on table **??** our observationally-comparable results for MHD halos at two important radii one corresponding to the approximate regimes where the MW DM halo is usually constrained.

Little discussion: Are our results congruent with observations? at which radii, does the DM halo shape vary that much?. Which models are favored?

4.4 The rounding effect of baryons

From the previous characterization of radial shapes it is clear that MHD halos are rounder than DM halos (i.e. axial ratios are bigger) at every sampled radii. This can be compared on tables **??** and **??** or at the representative example on figure

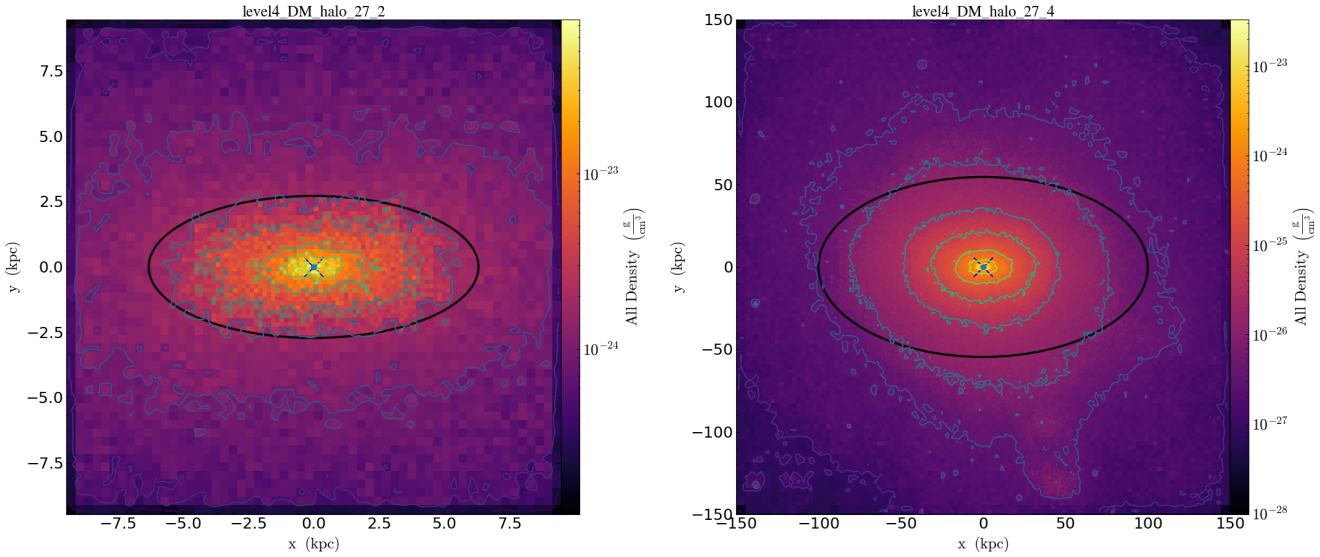

(a) halo 27 DM shape at small radius

(b) halo 27 DM shape at big radius

Figure 1. DM density for inner/outer (left/right panel) DM halo regions.

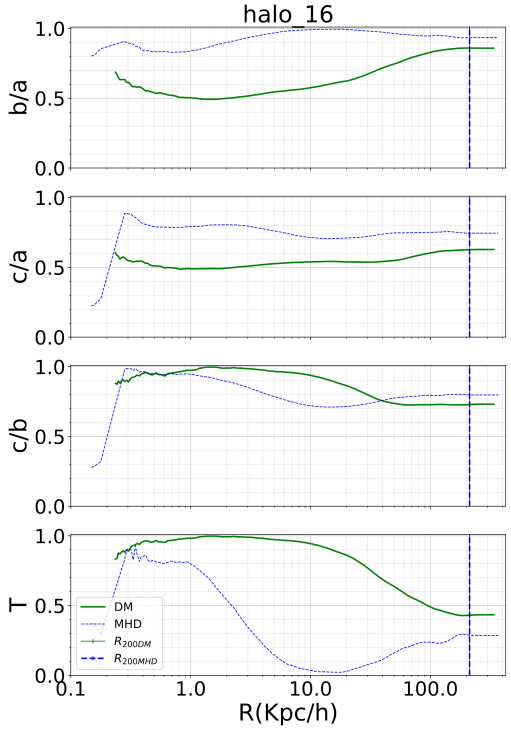

Figure 2. Radial profile for axial ratios and the triaxiality parameter $T = \frac{1-b/a}{1-c/a}$ for halo 16.

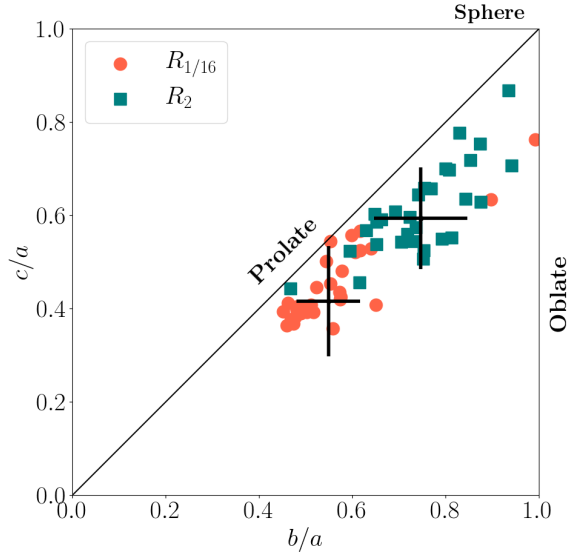

Figure 3. Shape of each halo on the plane c/a Vs b/a. Errorbar shows median and errors for each sampled radii.

??. From there, it is also noticeable that the rounding effect of baryons is stronger at the disk regime, where the DM halo is almost perfectly oblate. Furthermore, MHD halos tend towards more oblate shapes (T $<$ 0.5) despite DM halos tendency towards more prolate shapes (T>0.5).

This rounding effect is expected from the gravitational effect of the flattened axisymmetric galactic disk. It is also reasonable that this effect is not as strong at $\approx$ 100Kpc, where the disk potential is dimmer compared to the DM halo potential. Keeping this in mind, one would expect that the rounding effect of baryons is related to some galactic parameters such as its component masses and radii. However, even for the parameter of highest correlation with this rounding effect (the baryonic fraction), the relation is not clear nor conclusive due to the dispersion from galaxy peculiarities. In figure **??** we plot the ratios c/a compared to the baryonic fraction of each galaxy. Although some linear tendency is suggested qualitatively, the dispersion of the sample is very high to obtain some conclusive relation. This is an evidence that adiabatic-contraction models are not realistic

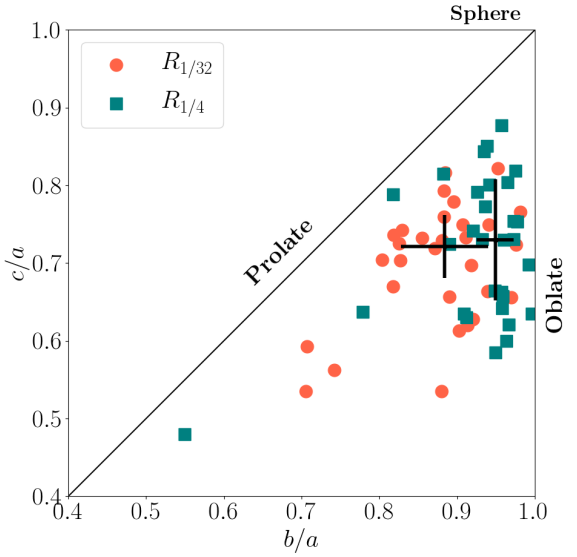

Figure 4. Shape of each halo on the plane c/a Vs b/a. Errorbar shows median and errors for each sampled radii.

asphericity Vs Star Density.png

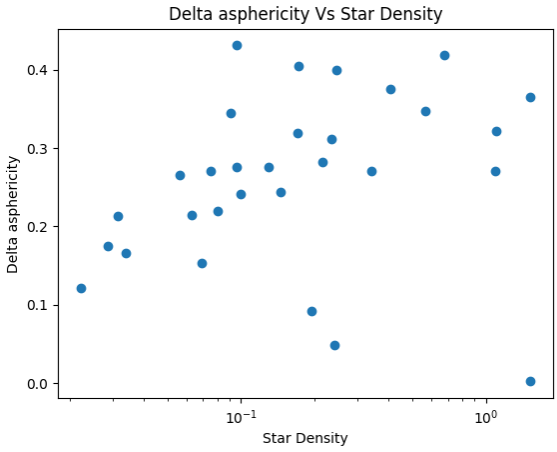

Figure 5. Difference in asphericities between MHD and DM shapes Vs Star Density of the simulation.

as they may neglect some effects of the galaxy evolution in the whole cosmological context.

Actually we have not examined the relation of c/a in MHD halos with some measure of c/a from the disk, that is something like Zdisk/Rdisk. This actually would make more sense from a physical point of view: effect of the potential.

Although the effect of the baryonic disk on the shape of the DM halo is a reasonable explanation for the rounding effect, it does not actually explain the deviation from oblateness of MHD halos at $r < 10$Kpc. In other words, if the disk is perfectly axisymmetric, there must be some source of triaxiality at $r < 10$Kpc to explain the low axial ratios.

Talk about source of triaxiality at the inner parts of the halos (bar?). This source of triaxiality at the inner parts explains why the axial ratios are ≈ 0.95 *and not exactly* 1. *We should also discuss that the decrease in the axial ratios for bigger radii may actually be bigger/steeper but it is dimmed by the contribution of inner parts.*

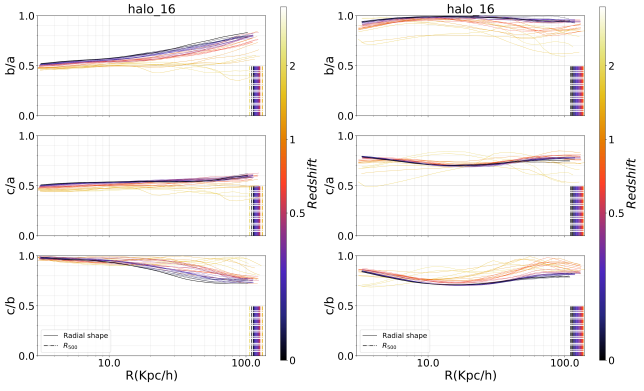

(a) halo 16 DM (b) halo 16 MHD

Figure 6. Radial profile (comoving) of axial ratios for halo 16 in terms of redshift (color). This halo maintains its shape until $z \approx 1$ obviating the systematic rounding effect in time from asymmetric potentials.

4.5 The historical shape

One of the principal motivations to study the radial dependence of the DM halo shape is that it may encode some clues about its formation history. We have already shown that DM-only halos seem to exhibit a steady and monotonous growth in its axial ratios when sampled at bigger radii. One similar effect can be found if we sample the shape at the virial radius, this time at varying redshift. It is easy to see that the axial ratios increase with decreasing redshift, which is expected by the continuous influence of the gravitational potential **?**. In figure **??** we present a representative example.

Interestingly, these two parametic plots i.e. $(b/a, c/a)(z = 0, r)$ and $(b/a, c/a)(z, r = R_{vir})$ are very correlated for DM-only halos **??**. This means that, for DM-only halos, one can approximate its shape at higher redshift by simply sampling its current shape at a smaller radius **wording**. This relationship relies strongly on the steady and monotonous tendency of DM halos towards sphericity for bigger radii and smaller redshift.

MHD halos, on the other hand, do not exhibit tendency towards sphericity with bigger radii, but they do get sistematically rounder at lower redshift as seen in figure **??**. This effectively vanishes this correlation as seen from a DM halo **??**.

Better graphics.

4.6 The orientation of the principa axes

One of the principal assumptions of observational models of the MW's DM halo is that its minor axis is perfectly aligned with the disk axis. Although this is a reasonable assumption to guarantee the stability of the galactic disk in simplified models of isolated galaxies, it may not be the case

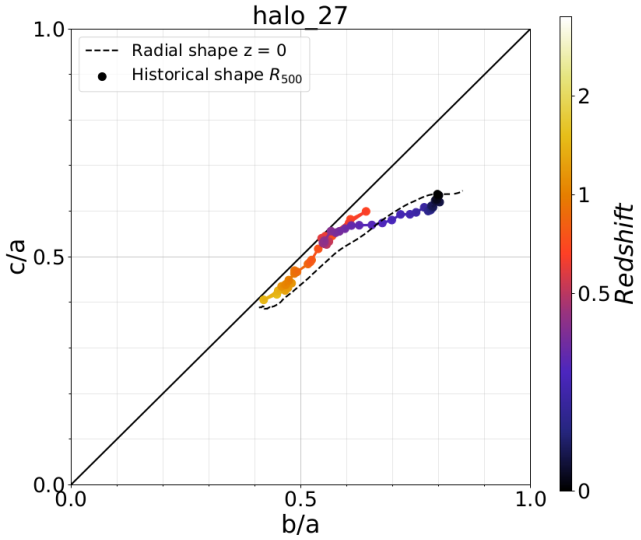

Figure 7. Difference in asphericities between MHD and DM shapes Vs Star Density of the simulation.

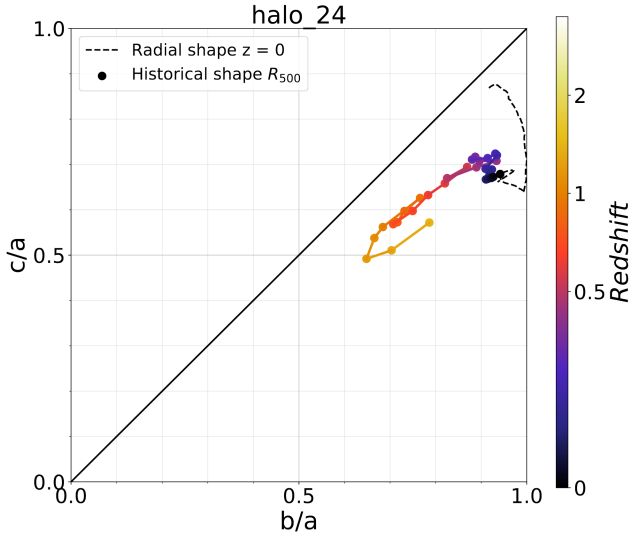

Figure 8. Difference in asphericities between MHD and DM shapes Vs Star Density of the simulation.

for galaxies evolved in the whole cosmological context nor at every radii at which the shape is sampled.

Therefore, it is of special interest to us to examin the strength of this alignment assumption in the context of simulations. For this purpose, we sampled the shape at 5 different radii and plotted the axial directions, as well as the disk direction in the **name** diagrams (explain diagrams). Explain disk direction calculation.

We found that there is not a representative example of what happens in terms of alignments. We found that the majority of the disks are aligned with the minor axis of their DM halo within $\approx 30^o$; in some special cases, this alignment was almost perfect and in some other cases, the DM halo minor axis changed substantially to be able to determine an alignment. In figure **??** we present these three cases. **occurrencies for each case?**

This is an important result of our study. We study the radial evolution of the principal axes, compared also to the angular momentum vector from the disk. We found that while the angular momentum tend to be aligned with the minor axis of the ellipsoid, this may not be the case all times. When there is an alignment it is usually within 20 degrees (get a histogram of this. and an evolution of this histogram with time). When there is not an alignment, then there is no simple way to determine towards which axis it is oriented. Furthermore, the principal axes alignment usually change with radius (rotation, swap, verify). This ask for relaxation on the strong constrains on the MW DM halo models.

Discussion about the distribution of alignments and their evolution in time: Precesion or temporary instabilities?

5 CONCLUSIONS

6 DISCUSSION

ACKNOWLEDGEMENTS

This project has received funding from the European UnionâĂŹs Horizon 2020 Research and Innovation Programme under the Marie Skłodowska-Curie grant agreement No 734374.

REFERENCES

Author A. N., 2013, Journal of Improbable Astronomy, 1, 1
Others S., 2012, Journal of Interesting Stuff, 17, 198

APPENDIX A: SOME EXTRA MATERIAL

If you want to present additional material which would interrupt the flow of the main paper, it can be placed in an Appendix which appears after the list of references.

This paper has been typeset from a TEX/LATEX file prepared by the author.

REFERENCES

Abadi M. G., Navarro J. F., Fardal M., Babul A., Steinmetz M., 2010, MNRAS, 407, 435
Allgood B., Flores R. A., Primack J. R., Kravtsov A. V., Wechsler R. H., Faltenbacher A., Bullock J. S., 2006, MNRAS, 367, 1781
Banerjee A., Jog C. J., 2011, ApJ, 732, L8
Bovy J., Bahmanyar A., Fritz T. K., Kallivayalil N., 2016, ApJ, 833, 31
Bowden A., Evans N. W., Williams A. A., 2016, MNRAS, 460, 329
Bryan S. E., Kay S. T., Duffy A. R., Schaye J., Dalla Vecchia C., Booth C. M., 2013, MNRAS, 429, 3316
Chua K. E., Pillepich A., Vogelsberger M., Hernquist L., 2018a, preprint, (arXiv:1809.07255)
Chua K. E., Pillepich A., Vogelsberger M., Hernquist L., 2018b, preprint, (arXiv:1809.07255)

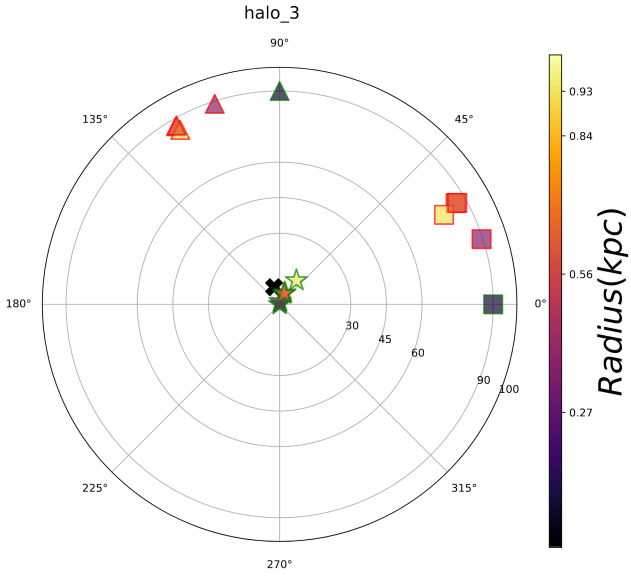

(a) Perfectly aligned Axes

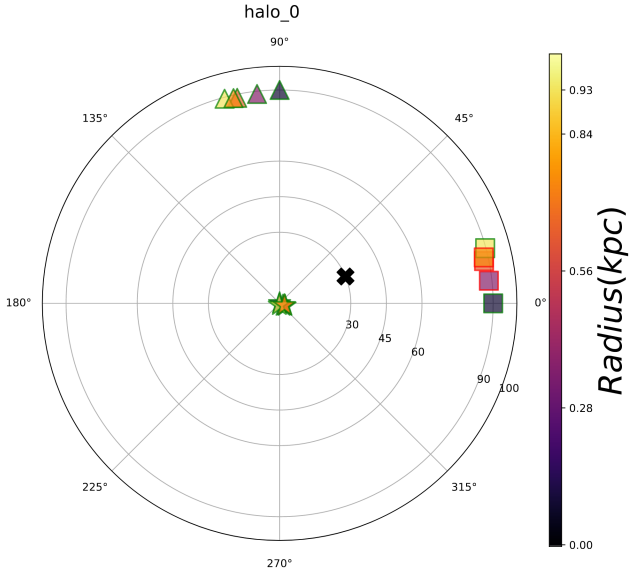

(b) Somewhat aligned Axes

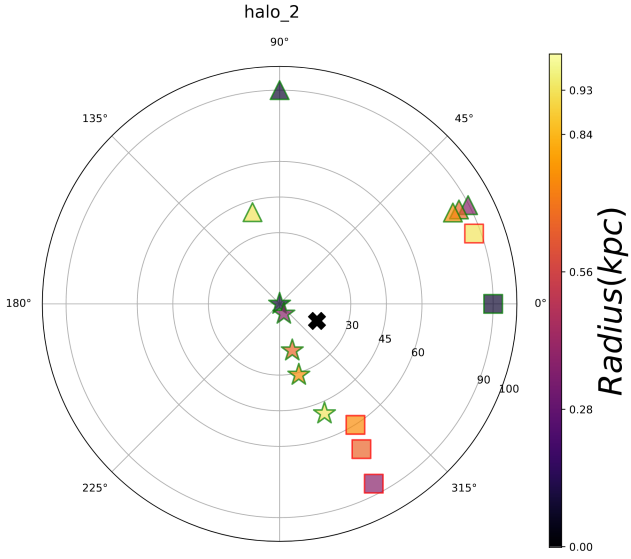

(c) Chaotic Axes

Figure 9. Description of axes alignments

Debattista V. P., Moore B., Quinn T., Kazantzidis S., Maas R., Mayer L., Read J., Stadel J., 2008, The Astrophysical Journal, 681, 1076
Debattista V. P., Roškar R., Valluri M., Quinn T., Moore B., Wadsley J., 2013, MNRAS, 434, 2971
Deg N., Widrow L., 2013, MNRAS, 428, 912
Grand R. J. J., et al., 2017, Monthly Notices of the Royal Astronomical Society, 467, 179
Ibata R., Lewis G. F., Martin N. F., Bellazzini M., Correnti M., 2013, ApJ, 765, L15
Johnston K. V., Law D. R., Majewski S. R., 2005, ApJ, 619, 800
Kazantzidis S., Abadi M. G., Navarro J. F., 2010, ApJ, 720, L62
Law D. R., Majewski S. R., 2010, The Astrophysics Journal, 714, 229
Law D. R., Majewski S. R., Johnston K. V., 2009, The Astrophysical Journal Letters, 703, L67
Loebman S. R., Ivezić Ž., Quinn T. R., Governato F., Brooks A. M., Christensen C. R., Jurić M., 2012, ApJ, 758, L23
Olling R. P., Merrifield M. R., 2000, MNRAS, 311, 361
Pearson S., Küpper A. H. W., Johnston K. V., Price-Whelan A. M., 2015, ApJ, 799, 28
Schaye J., et al., 2015, Monthly Notices of the Royal Astronomical Society, 446, 521
Springel V., 2010, Monthly Notices of the Royal Astronomical Society, 401, 791
Vera-Ciro C., Helmi A., 2013, ApJ, 773, L4
Vera-Ciro C. A., Sales L. V., Helmi A., Frenk C. S., Navarro J. F., Springel V., Vogelsberger M., White S. D. M., 2011, MNRAS, 416, 1377